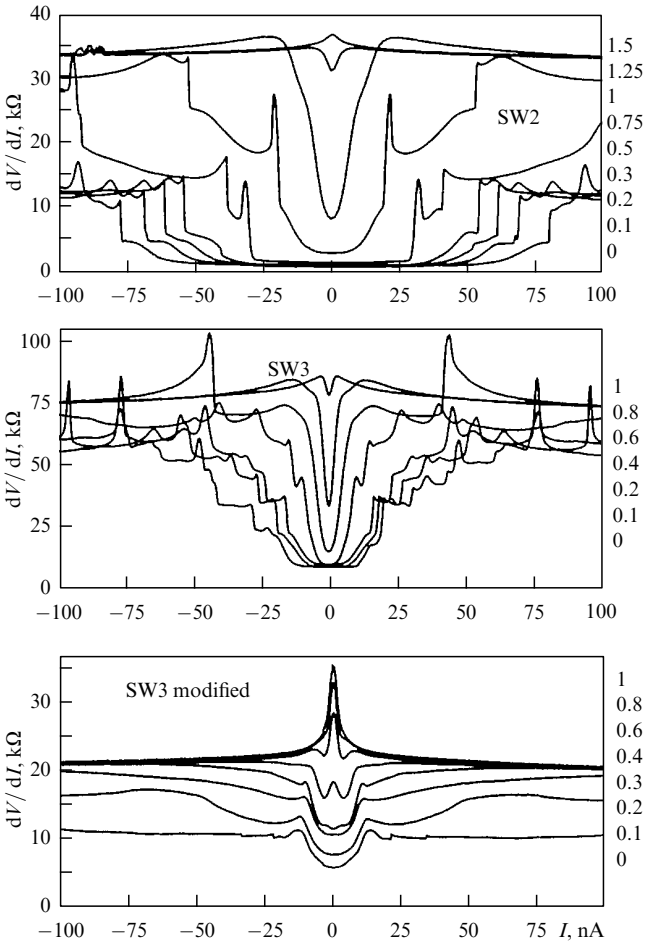

Figure 3. Dufferential resistance as a function of current for samples SW2, SW3 and SW3m, at $T = 70$ mK. (Fields are indicated in Teslas to the right of the curves).

References

1. Greene R B R L et al. *Phys. Rev. Lett.* **34** 577 (1975); Jerome D et al. *J. Phys. Lett.* (Paris) **41** L95 (1980)
2. Kasumov A Yu et al. *Science* **284** 1508 (1999)
3. Morpurgo A F et al. *Science* **286** 263 (1999)
4. Schon G *Nature* **404** 948 (2000); Zaikin A D et al. *Usp. Fiz. Nauk* **168** 244 (1998) [*Phys. Usp.* **41** 226 (1998)]; Zaikin A D et al. *Phys. Rev. Lett.* **78** 1552 (1997)
5. Bezryadin A et al. *Nature* **404** 971 (2000)
6. Kasumov A Yu et al. *Europhys. Lett.* **34** 429 (1996); Kasumov A Yu et al. *Europhys. Lett.* **43** 89 (1998)
7. Dujardin E et al. *Solid State Commun.* **114** 543 (2000)
8. Ando T et al. *J. Phys. Soc. Jpn.* **67** 2857 (1998)
9. Bachtold A et al. *Phys. Rev. Lett.* **84** 6082 (2000)
10 Ebessen T W et al. *Nature* **382** 54 (1996)
11. Bogomolov V N et al. *Solid State Commun.* **46** 383 (1983)
12. Joyez P et al. *Phys. Rev. Lett.* **72** 2458 (1994)
13. Kasumov A Yu et al. *Science* **291** 280 (2001)

Scanning tunneling spectroscopy on superconducting proximity nanostructures

C Chapelier, M Vinet, F Lefloch

Abstract. We investigated the local density of states (LDOS) of a normal metal (N) in good electrical contact with a superconductor (S) as a function of the distance x to the NS interface. The sample consists of a pattern of alternate $L = 1$ μm wide strips of Au and Nb made by UV lithography. We used a low temperature scanning tunneling microscope and a lock-in detection technique to record simultaneously $\mathrm{d}I/\mathrm{d}V(V, x)$ curves and the topographic profile $z(x)$ at 1.5 K. We scanned along lines perpendicular to the strips. All the spectra show a dip near the Fermi energy, which spectral extension decreases from the superconducting gap Δ at the NS interface to zero at distances $x \gg \xi_N$ where $\xi_N \simeq \sqrt{\hbar D_N/2\Delta} \simeq 53$ nm is the coherence length in the normal metal. Our measurements are correctly described in the framework of the quasi-classical Green's function formalism. We numerically solved the 1D Usadel equation and extracted a decoherence time in gold of 4 ps. We also investigated the LDOS of small ridges of Au deposited on the top of the Nb lines. In this case, $L \leq \xi_N$ and the spatial variations of the spectra depend on the exact shape of the Au ridge. However, our results are consistent with a predicted minigap related to the Thouless energy.

1. Introduction

It is actually believed that all the experiments on normal metal – superconductor (NS) heterostructures can be understood from a unified point of view based on the theory of non-equilibrium superconductivity [1, 2]. The underlying Usadel [3] equations governing this proximity effect introduce a coherence length $\xi_N \simeq \sqrt{\hbar D_N/2\Delta}$ (Δ is the superconducting gap and D_N is the diffusion coefficient of the N metal). Depending on the ratio L/ξ_N where L is the size of the N metal, different behaviors are predicted [2]. On the one hand, when $L \gg \xi_N$ (infinite system), the superconducting correlations induced in N lead to a depression of the electronic density of states around the Fermi energy E_F. The energy scale of this dip in the LDOS vanishes to zero at increasing distances from the NS interface. On the other hand, when L is comparable to ξ_N (finite system) the LDOS shows a space independent minigap E_g whose width is related to the Thouless energy $E_{Th} = \hbar D/L^2$.

Several experiments address the spatial variations of the LDOS either in the infinite case at a scale larger than ξ_N [4] or with a much higher resolution but only in a finite geometry [5 – 7]. We report here measurements of the LDOS by scanning tunneling spectroscopy on Nb/Au proximity junctions. Since STM allows a high energetic and spatial resolution in conjunction with sample topography we are able to spatially resolve the LDOS in the normal metal as a function of the distance x to the NS interface (x can vary from zero to several coherence lengths with a resolution of a few nanometers). Moreover, we can discriminate between the two situations: $L \leq \xi_N$ and $L \gg \xi_N$ within the same sample.

C Chapelier, M Vinet, F Lefloch Département de Recherche Fondamentale sur la Matière Condensèe, SPSMS, CEA-Grenoble — 17 rue des Martyrs, 38054 Grenoble Cedex 9, France

2. Experimental conditions

Our STM hangs inside a sealed tube by a one meter long spring to decouple it from external vibrations. This tube is immersed in a ^{4}He cryostat. Cooling is achieved by introducing high-purity helium exchange gas into the tube. The temperature is reduced to 1.5 K by pumping on the helium bath. Tunneling spectra are obtained by a lock-in detection technique with a 77 μV peak-to-peak modulation voltage of the bias at 1 kHz. We measure the differential conductance $\mathrm{d}I/\mathrm{d}V$ versus V while holding the STM tip at a fixed height above each position $\mathbf{r}$. This provides a local probe of the LDOS $n(eV, \mathbf{r})$. The energetic resolution is determined by the thermal broadening at 1.5 K. Each curve is a single acquisition process with no additional averaging. The $\mathrm{d}I/\mathrm{d}V$ curves and the topography are measured during the same line scan allowing us to correlate them precisely. Data are normalised to the conductance at high voltage ($V > \Delta$). The same normalization coefficient has been used for all the curves. The typical tunneling resistance is 10^7 Ω.

We have chosen Au as a normal metal because it is chemically inert. The Au film has been previously characterized by measuring the temperature dependence of the resistivity, $R(T)$, which gives the mean free path $l_N \simeq 22$ nm. Nb is used as a superconductor because of its high critical temperature. Our 50 nm thick Nb film undergoes a BCS transition at 8.1 K and shows an energy gap $\Delta \simeq 1.15$ meV at 1.5 K.

Our sample consists of a 50 nm thick pattern of juxtaposed strips, 1 μm wide and 250 μm long, of Au and Nb in good electrical contact, see Figs 1a, b. The Nb strip was first uniformly deposited by DC sputtering on a thermally oxidized Si wafer. We used UV lithography and subsequent reactive ion etching (RIE) to produce the Nb strips. Ten percent of oxygen was introduced in the SF_6 plasma during RIE in order to remove all organic residues and to give some inclination to the edges of the Nb strips (see Fig. 1b where this inclination has been a lot exaggerated). This ensures an NS interface over the full height of the layers. We then sputtered 2 nm Ti and 50 nm Au to fill up the grooves between the Nb strips and lifted-off the remaining resist. Prior to the Ti/Au sputtering the Nb surface has been cleaned and the native oxide removed by an *in situ* inverse plasma shallow etching to ensure a good metallic contact. As seen in Figs 1a, c, Au forms ridges on each side of the Nb strips. The size of these ridges has been measured both by STM and scanning electron microscopy. Their lateral dimensions vary from 50 nm to 200 nm and their heights from 10 nm to 50 nm. They are in electrical contact with Nb but poorly connected to the rest of Au. Indeed, we observe BCS-like $\mathrm{d}I/\mathrm{d}V(V)$ curves in between the Au ridges and the Au strips, which indicates the presence of bare Nb. We can fit these spectra with Dyne's formula with a complex energy $E^* = E - \mathrm{i}\Gamma$, where Γ reflects the finite lifetime of quasi-particles [8]. In contrast, spectra taken above Au either over the ridges or the strips cannot be fitted using this model. This allows us to infer the NS interface.

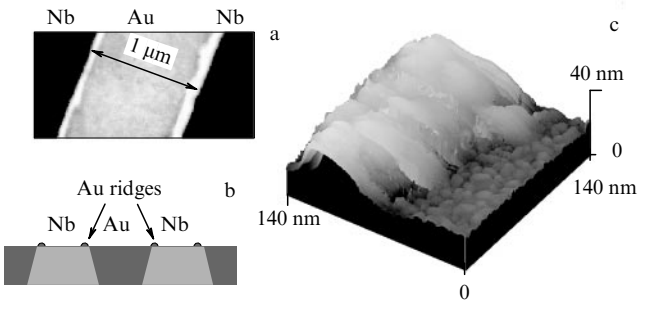

Figure 1. (a) Scanning electron microscope photography of the sample displaying the small ridges on each side of the Au strip. (b) Schematic cross-section of the sample. It consists of a 50 nm thick pattern of self aligned strips, 1 μm wide and 250 μm long, of Au and Nb. (c) A 140 nm × 140 nm × 40 nm topographic STM picture of a Au ridge.

3. Results

3.1 Case $L \gg \xi_N$.

In the first set of experiments we scanned above the Au strip surface and measured the LDOS as a function of the distance x from the NS interface. The spectra were taken along the same line perpendicular to the interface and x was varied from zero to several hundreds of nm by steps of 2 nm. As an example, three of them are displayed in Fig. 2a for three distances. We observe a peak in $G_V(x) = \mathrm{d}I/\mathrm{d}V(V, x)$ at an energy $\varepsilon_{\max}$ which decreases as we move away from the superconductor. Figures 2c,d display the normalised zero-bias conductance $g = G_{V=0}/G_{V=4\ \mathrm{mV}}$ (open circles) and $\varepsilon_{\max}$ (solid squares) as a function of x. A zero density of states at the Fermi level is never observed due to pair-breaking mechanisms such as spin-flip and inelastic scattering which cannot be neglected at 1.5 K.

We describe our results with the help of the 1D-diffusion Usadel equation [3]:

$$\frac{\hbar D}{2}\frac{\partial^2\theta}{\partial x^2} + (\mathrm{i}E - \Gamma_{\mathrm{in}} - 2\Gamma_{\mathrm{sf}}\cos\theta)\sin\theta + \Delta(x)\cos\theta = 0\,, \tag{1}$$

where Γ_{sf} and Γ_{in} are the spin-flip and the inelastic scattering rates, respectively, $\Delta(x)$ is the pair potential. The LDOS n of

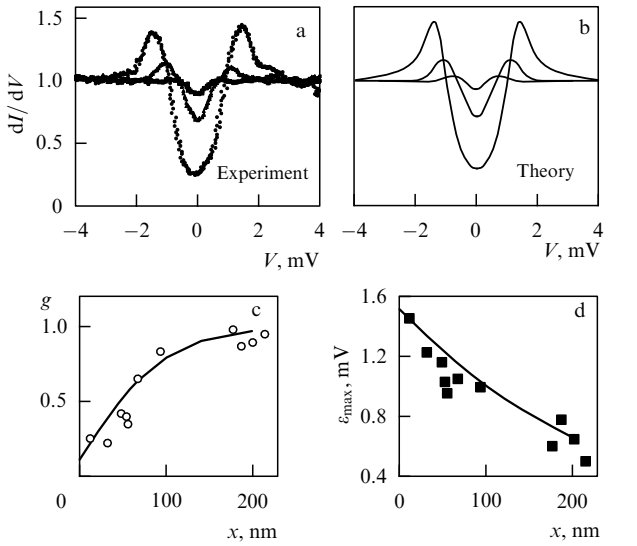

Figure 2. (a) Measured spectra at 20, 75 and 195 nm from the interface. (b) Calculated spectra at 20, 80 and 160 nm. (c) and (d) represent, respectively, the normalized zero-bias conductance g and the energy of the peak $\varepsilon_{\max}$, as functions of the distance x to the NS interface. The solid lines correspond to the fit.

the quasi-particles is related to θ by

$$n(E,x) = n_0 \,\mathrm{Re}[\cos\theta(E,x)]\,.$$

Close to the NS interface the order parameter is space-dependent and obeys a self-consistent equation [1, 2]. However, for the sake of simplicity we assume no pair potential in the normal metal ($\Delta_N = 0$) whereas we take Δ equal to its bulk value everywhere in the superconductor. Conditions of continuity $\theta_{x=0^-} = \theta_{x=0^+}$ and spectral current conservation $\sigma_S(\partial\theta/\partial x)_{x=0^-} = \sigma_N(\partial\theta/\partial x)_{x=0^+}$ are imposed at the NS interface, which is valid in the case of a perfect electrical contact. This assumption is justified by the careful cleaning of the Nb surface prior to the normal films deposition. However, the presence of Ti and the possible alloying of the different metals complicate a lot the actual interface description. We therefore choose to introduce an effective conductivity σ_{Neff} instead of the gold one σ_N. We compare our measurements to the convolution of the LDOS calculated from Usadel equations with a Fermi – Dirac distribution. As can be seen on Figs 2a,b, the calculated spectra at distances 20, 80 and 160 nm are very similar to the experimental ones taken at $x = 20$, 75 and 195 nm with $\sigma_S/\sigma_{Neff} = 4$ and $\xi_N = 100$ nm. The solid lines in Figs 2c,d represent the computed values of the peak position ε_{max} and of the zero-bias conductance g.

Moreover, the fits are sensitive in different ways to the two scattering rates. We find that while Γ_{in} can be neglected ($\Gamma_{in} < 0.01\Delta$), the phase decoherence in our Au film is dominated by the spin-flip mechanism. We obtain a spin-flip time $\tau_{sf} = \hbar/\Gamma_{sf} = 4$ ps in good agreement with recent experiments [9]. However, these latter measurements are unable to identify the decoherence mechanism. It should be therefore interesting to reproduce our results at a lower temperature. This may enlighten in a new way the controversy about the saturation of the coherence time in diffusive metals.

3.2 Case $L \leq \xi_N$.

During the sample fabrication, small ridges of Au build up on each side of the Nb strips as can be seen in Fig. 1. Their dimensions vary from 10 nm to 50 nm. In the second step of experiments, we have investigated the LDOS over these small ridges. In this configuration, we find that the position of the peaks in $\mathrm{d}I/\mathrm{d}V(V,x)$ does not depend on the distance to the NS interface, in striking contrast to the preceding case. For a ridge of 20 nm height, we observe that the maximum is located at 1.5 meV (see Fig. 3) whereas for a ridge of height 50 nm, the position of the peak is 0.95 meV (see Fig. 4). Theoretically, in such a finite diffusive geometry, i.e. when $L \simeq \xi_N$, a minigap E_g is predicted in the LDOS. E_g is related to the Thouless energy $E_{Th} = \hbar D_N/L^2$. Although we only measure the position of the peaks and not E_g (due to the strong spin-flip scattering, there is no true minigap in our system), our results are consistent with the expected behavior of the minigap as a function of the size L.

The evolution of the normalised zero-bias conductance with x is different for the two ridges. In the bigger one, the LDOS suddenly changes as soon as the tip probes the Au surface and remains identical for any location above the ridge whereas in the smaller one, g continuously increases with x from 0.1 to 0.9. We believe that this difference is related to the shape of the ridge. However, it should also be noted that the size of the ridges is of the same order of magnitude as the elastic mean free path and that the quasi-ballistic regime is beyond the Usadel equation validity.

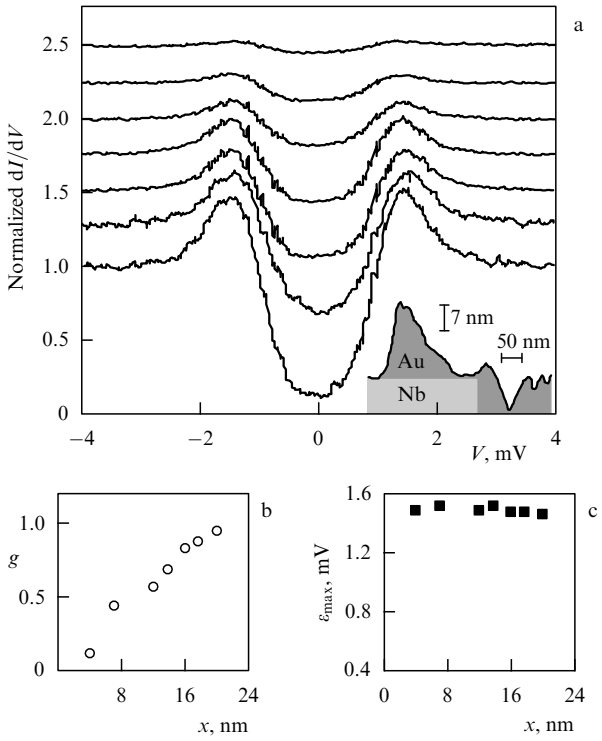

Figure 3. (a) Spectra taken at different positions above a ridge 20 nm high. The curves have been evenly shifted for clarity. The lower curve has been taken at the bottom of the ridge and the upper one at the top of it. The inset is an STM profile of the ridge. (b) Normalized zero-bias conductance, $g = G_{V=0}/G_{V=4\,mV}$ as a function of the distance x to the NS interface. (c) Energy of the peaks, ε_{max}. While g continuously increases with x, $\varepsilon_{max} = 1.5$ meV does not vary.

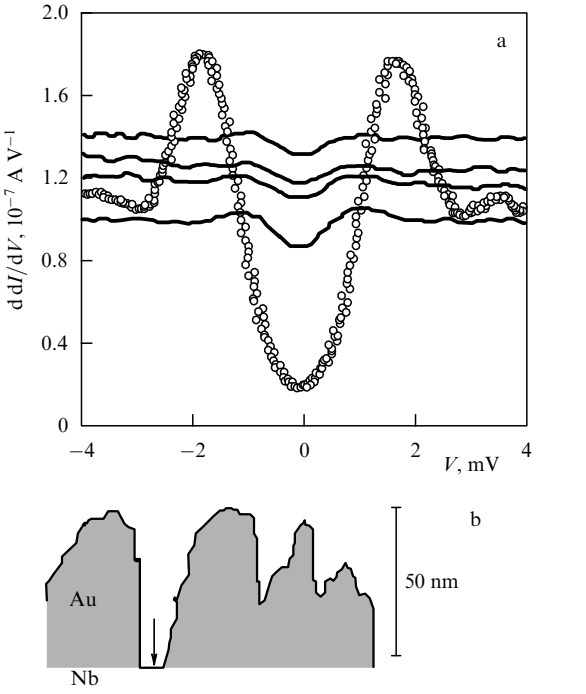

Figure 4. (a) Spectra taken at different positions above a ridge 50 nm high. The curves have been evenly shifted for clarity; $\varepsilon_{max} = 0.5$ meV. The open dots curve has been taken on top of Nb at the location pointed by the arrow on Fig. (b). (b) is an STM profile of the ridge.

4. Conclusions

In summary, we have probed the proximity effect in two different systems. First, we have investigated the LDOS of a semi-infinite normal metal and found space-dependent energy spectra as a function of the distance to the NS interface. This behavior is in good agreement with the pseudo-gap model predicted by the theory of non-equilibrium superconductivity. But STM techniques allow also to address much smaller scales. Indeed, we have simultaneously investigated the local density of states in a confined geometry. In this case we have found a spectral structure which does not vary in space and which can be related to the Thouless energy. Similar experiments are under way at very low temperature in a dilution refrigerator. This should give more information on the temperature dependence of the scattering rates in the infinite case and on the value of the minigap in the finite one.

References

1. Bruder C *Supercond. Rev.* **1** 261 (1996); Volkov A F, Zaitsev A V, Klapwijk T M *Physica C* **210** 21 (1993); Golubov A A, Wilhelm F K, Zaikin A D *Phys. Rev. B* **55** 1123 (1997)
2. Belzig W, Bruder C, Schön G *Phys. Rev. B* **54** 9443 (1996)
3. Usadel K D *Phys. Rev. Lett.* **25** 507 (1970)
4. Guéron S et al. *Phys. Rev. Lett.* **77** 3025 (1996)
5. Tessmer S H, Van Harlingen D J *Phys. Rev. Lett.* **70** 3135 (1993); Tessmer S H et al. *Phys. Rev. Lett.* **77** 924 (1996)
6. Truscott A D, Dynes R C, Schneemeyer L F *Phys. Rev. Lett.* **83** 1014 (1999)
7. Levi Y et al. *Phys. Rev. B* **58** 15128 (1998)
8. Dynes R C, Narayanamurti V, Garno J P *Phys. Rev. Lett.* **41** 1509 (1978)
9. Gougam A B et al. *J. Low Temp. Phys.* **118** 447 (2000)

Quantum entangled states and reduction of the wave packet

G B Lesovik

Abstract. The paper deals with entangled electron states arising in a normal conductor located near a superconductor. Such paired entangled states can be treated as decomposed Cooper pairs. Some general problems of the theory of measurements are also considered.

1. Introduction

In recent years quantum entangled states have attracted considerable interest of experimenters and theoreticians, for which there are several reasons. On the one hand, the states can be used in quantum cryptography and in quantum computers. On the other hand, they are related to fundamental problems of the theory of measurements and to the possibility to verify the existence of hidden variables and nonlocal character of quantum mechanics, etc.

The entangled states of two (or more) particles can be defined as follows: the states are referred to as entangled if two-particle probabilities describing the system do not reduce to the product of the corresponding one-particle probabilities.

Let us consider, for example, the system of two spins, whose absolute value is equal to 1/2. When $P_{+-} \neq P_{+}P_{-}$, the states are entangled. In particular, this means that the measurement of one spin affects *apriori* the probability of another spin.

The effect is especially surprising when two spins are spaced, and the expected time of measurements is much less than the time during which a light signal goes from one spin to another. It is just this phenomenon that has led to the conclusion about nonlocal character of quantum mechanics.

A gedanken experiment of this type was first considered by Einstein, Podolsky, and Rosen (EPR). As for real experiments with photons, they have been carried out only recently.

Some theoretical schemes for obtaining entangled electron states have been suggested this year [1, 2].

In Reference [2], an experiment with electron in the NS system was proposed. The main concept is simple and based on the use of Cooper pairs emitted by a superconductor into a normal metal in the form of EPR pairs. The superconductor is connected with two normal conducting wires. One or two electrons can be emitted into each conducting wire. To split the electron pair along 'arms' and to avoid entering of both the electrons into the same load, the contacts contain filters. The electrons in a pair are correlated by two variables, i.e., by the kinetic energy and the spin so that the energy of one electron is slightly higher and that of the other one is slightly less than the Fermi energy, while the electron spins are opposite (at s-pairing). Therefore, the filters can treat either the difference in kinetic energy or the difference in spins. In the first case, the electrons can be splitted with interferometers based on quantum dots, while in the second case — with interferometers based on ferromagnetic contacts. (In Ref. [3] it was suggested to use quantum dots, whose sizes are rather small to prevent tunneling of both the electrons due to high value of the Coulomb energy, as filters.) In order to detect the entanglement, it is proposed to study the correlators of the number of electrons entering each arm. The correlator of the number of electrons recorded during a long period t is expressed in terms of current correlators at zero frequency as $\langle\langle N_1 N_2\rangle\rangle = t\langle\langle I_1 I_2\rangle\rangle$.

Thus, the experimental task is to measure current correlator at low frequency. In the case of ideal filters the correlators are positive and their absolute values are equal to autocorrelators in each contact: $\langle\langle I_1 I_2\rangle\rangle = \langle\langle I_2 I_2\rangle\rangle = \langle\langle I_1 I_1\rangle\rangle$.

Note that the entangled states can be different. In particular, the singlet state is entangled at any orientation of the axis of measurements, while for the triplet state there is a direction at which the measurements yield single-valued data. In our scheme with ferromagnetic filters, the effect could be checked by varying the polarization of ferromagnetics.

2. Measurements and reduction of the wave packet

Most of physicists believe that the EPR experiment implies that quantum mechanics is not local. The experiments on photons are considered to prove this standpoint, although some recent publications point to several logic loop-holes in these experiments, if we treat them as evidence in favor of the absence of hidden variables. The key qualitative effect being verified in this case is the so-called Bell inequality.

G B Lesovik L D Landau Institute for Theoretical Physics, Russian Academy of Sciences, ul. Kosygina 2, 117940 Moscow, Russian Federation